Asian Journal of Physics
Vol. 29, Nos 10-12 (2020) 797-803
Available on: www.asianjournalofphysics.in

Convolutional neural network based fringe pattern denoising algorithm

D Bhatt[1], R Kulkarni[2], and P K Rastogi[3]
[1]*Department of Electrical Engineering ,*
National Institute of Technology Surat -395 007, India.
[2]*Department of Electronics and Electrical Engineering*
Indian Institute of Technology Guwahati, Guwahati-721 009, Assam, India.
[3]*Applied Computing and Mechanics Laboratory,*
Ecole Polytechnique Fédérale de Lausanne (EPFL), Lausanne, Switzerland.

This article is dedicated to Prof FTS Yu for his significant contributions to Optics and Optical information Processing

Fringe pattern denoising is a crucial pre-processing operation in the fringe analysis procedure for obtaining reliable quantitative measurements in an optical interferometric setup. A convolutional neural network based fringe denoising algorithm is proposed considering a simple model architecture. The network training is performed using fringe patterns generated with random phase profiles. The corresponding noisy fringe patterns are generated using multiplicative speckle noise model in order to simulate the practical fringe pattern recording process. The algorithm is designed such that arbitrary sized fringe pattern denoising can be performed. Simulation and experimental results are provided for performance comparison of the proposed algorithm with some representative *State-of-Art* techniques. The results substantiate the effectiveness of the proposed algorithm in practical applications.

Keywords: Fringe pattern denoising, Convolutional neural network, Speckle noise, Optical interferometry.

1 Introduction

Optical interferometric techniques such as holographic interferometry, electronic speckle pattern interferometry (ESPI), and shearography are used in precision measurement applications [1-3]. In these techniques, the information on the measurand is recorded in the form of a fringe pattern which basically represents sinusoidal variations in the intensity of the interference field. Although the spatial variation in the measurand can be observed using the fringe pattern, it is only possible in a qualitative manner. Consequently, fringe pattern demodulation is essential for extracting the quantitative information on the measurand. Over the years, a number of fringe demodulation techniques have been proposed in the literature. In general, fringe patterns are severely corrupted by speckle noise, which is multiplicative in nature, on account of the coherent light source used in the interferometric setup. The presence of speckle noise is a major impediment in the fringe pattern demodulation process. Therefore, fringe pattern denoising is an essential pre-processing step for reliable fringe pattern demodulation.

A number of fringe denoising algorithms have been reported, for example, techniques based on moving average/median filter, spin filter [4,5], partial differential equations (PDEs) [6-8] and transform based techniques such as Fourier transform [9], wavelet transform [10-12], and windowed Fourier transform [13], dimensionality reduction [14], empirical mode decomposition [15], and non-local filter [16]. Performance comparison of different fringe denoising techniques have also been provided in [17,18].

Corresponding author :
e-mail: rishi.k@iitg.ac.in (Rishikesh Kulkarni);

Recently, machine learning algorithms have been applied for the fringe pattern analysis. For example, fringe denoising methods based on convolutional neural networks have been reported in [19-23]. In this paper, we propose a fringe denoising algorithm based on convolutional neural network (CNN) considering a simple model architecture.

2 Theory

Let us consider the generation of fringe patterns in a typical optical interferometric setup. Initially, an intensity of the interference between the reference light beam and the light beam associated with the object under investigation is recorded. A typical intensity pattern corresponding to reference state of the object can be represented as

$$I_1(x, y) = a(x, y) + b(x, y)\cos[\phi(x, y)],$$

where, (x, y) represents pixel coordinates; $a(x, y)$, $b(x, y)$ and $\phi(x, y)$ represent the background intensity (sum of individual intensities of reference and object beam), interference term amplitude and phase difference between the reference and object beam, respectively. In the case of optically rough objects, the phase values are uniformly distributed in the range of $(-\pi, \pi)$. As a result, an intensity pattern contains randomly distributed speckles. Upon external excitation, the object changes its reference state, which results in a deterministic change in the phase distribution. Let us represent the intensity pattern corresponding to the changed state of the object as

$$I_2(x, y) = a(x, y) + b(x, y)\cos[\phi(x, y) + \Delta\phi(x, y)],$$

where, $\Delta\phi(x, y)$ represents the deterministic change in the phase. A fringe pattern corresponding to the measurement of change in the object state is calculated as the absolute difference between the two intensity patterns as

$$\begin{aligned} I(x, y) &= |\, I_1(x, y) - I_2(x, y)\,| \\ &= 2\left|b(x, y)\sin[2\phi(x, y) + \Delta\phi(x, y)/2]\sin[\Delta\phi(x, y)/2]\right| \end{aligned}$$

It can be observed that the second sinusoidal component of the fringe pattern corresponds to the deterministic $\Delta\phi(x, y)$ and the first sinusoidal component of the fringe pattern acts as multiplicative noise source due to random nature of $\phi(x, y)$. In order to reliably extract the phase $\Delta\phi(x, y)$ from the fringe pattern, the fringe pattern contribution of the multiplicative noise component needs to be minimized. In the following, we describe the proposed CNN architecture designed for the purpose of fringe pattern denoising.

2.1 Model

In the proposed method, a simple CNN architecture is used with four convolution layers as shown in Fig 1. Whereas the first three layers generate 64 feature maps individually, the last convolution layer generates a single channel output. The convolution layers are followed by the BatchNorm (BN) operation and a nonlinear activation of LeakyReLU (negative slope = 0.01). The second and third convolution layers are followed by a 20% dropout operation. Each Conv2d layer has a *Kernel size* = (3, 3), *stride* = (1, 1) and padding = (1,1). A skip connection is given between the input layer and output of the fourth convolution layer to improve the flow of gradients. Kaiming weight from normal distribution is used for weight initialization of the network and bias was set to 0.01 for each layer. We utilize the most widely used loss function for image denoising operation based on mean-squared error (MSE) loss,

$$MSE = \frac{1}{N}\sum |I_f - I'|^2$$

where N represents no. of pixels. In each example of the training set, a speckle noise corrupted fringe pattern (I) is generated which is fed as an input of the network. The final output of the network (I_f) is compared pixel-wise against the ground-truth speckle-free image (I').

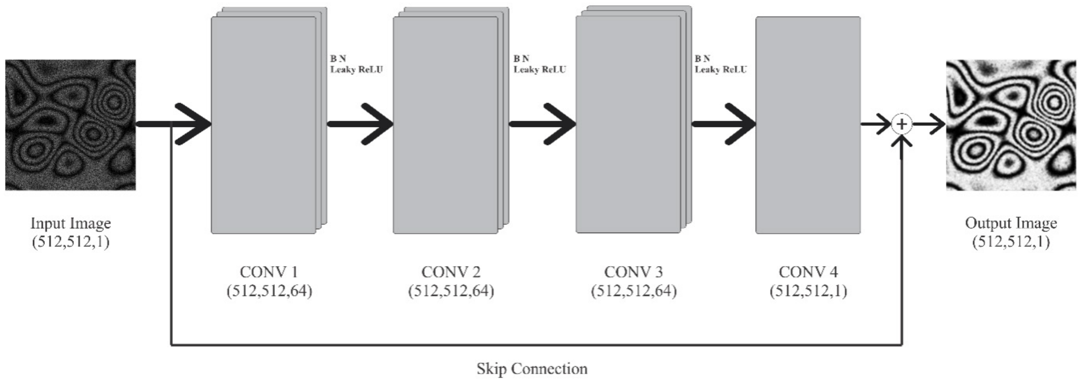

Fig 1. Convolutional neural network architecture considered in the proposed fringe pattern denoising approach.

2.2 Training and Model Output

The training data set consists of 5000 grayscale pairs of fringe patterns (noise-free and noisy) each of size 512×512 pixels. The validation set consists of 500 grayscale pairs of fringe patterns (each clean and noisy) of size 512×512 pixels. The fringe patterns were converted into tensors using pytorch's inbuilt transforms. The model is trained is performed with a learning rate of 0.01, a batch size of 1 and for 5 epochs (25,000 iterations). Adam optimizer is used for the optimization task of the model with the values of $\beta_1 = 0.9$, $\beta_2 = 0.999$, $\epsilon = 10^{-8}$. In order to operate with arbitrary sized speckle images, they are divided into patched of 512×512. Subsequently, the denoising procedure is applied to each patch. Finally, the noise-filtered outputs of the patches are combined together to generate an output image of the same size as that of the input image. It is important to note that no up-sampling or down-sampling operation of the image is performed in the entire model, thus eliminating any possible adverse effects associated with these operations.

3 Simulation and Experimental Results

Figure 2 shows three representative examples of noise-free fringe patterns in the first row and the associated speckle noise corrupted fringe patterns in the second row. Total 5000 number of such pairs are generated for the purpose of training the network. The network training was performed using the Google Colab platform. The training of the network approximately takes four hours with the desktop computer.

The denoising performance of the proposed method is compared with three fringe denoising techniques based on nonlinear PDE [6], windowed Fourier filtering (WFF) [13], and dimensionality reduction (DR) [14]. Two simulated speckle noise corrupted fringe patterns examples shown in Figs 3 (a) and 3 (b) are considered for the purpose of comparison. Figures 4 and 5 provide visual comparison of denoising results corresponding to Figs 3 (a) and 3 (b), respectively. It can be noted that the proposed algorithm provides improved denoising performed compared to other *State-of-Art* methods. For the quantitative comparison of these techniques, we consider two performance metrics defined in [10]. First metric, image fidelity (IF), is defined as

$$IF = 1 - \frac{\sum (I - I_f)^2}{\sum I^2}$$

and second metric, *speckle index* (SI) as,

$$SI = \sum \frac{\sigma_{I_{f(x,y)}}}{\mu_{I_{f(x,y)}}}$$

where, $\sigma_{I_{f(x,y)}}$ and $\mu_{I_{f(x,y)}}$ represent local standard deviation and mean of the fringe image computed within for example, 5×5 windows, respectively. The speckle index basically indicates the local smoothness of the filtered fringe pattern. That is, a lower speckle index corresponds to a higher amount of speckle denoising and vice - versa. Table 1 provides quantitative comparison of denoising algorithms corresponding to the fringe patterns given in Figs 3 (a) and 3 (b). The proposed algorithm provided highest image fidelity and lowest speckle index for both the examples. The performance with respect to speckle index can be improved with increased network complexity and number of training examples.

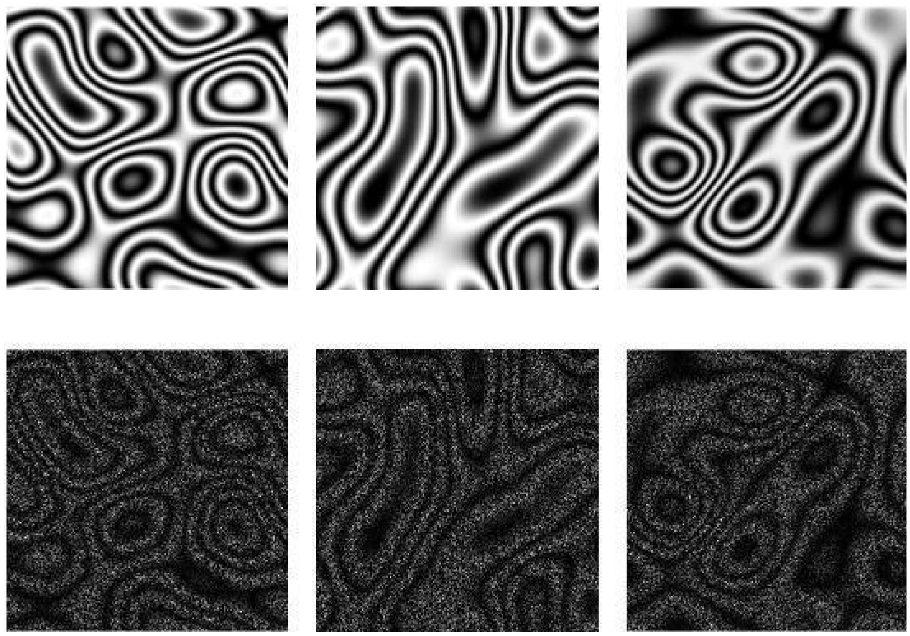

Fig 2. Network training data set: first row: noise-free fringe patterns; second row: noisy fringe patterns.

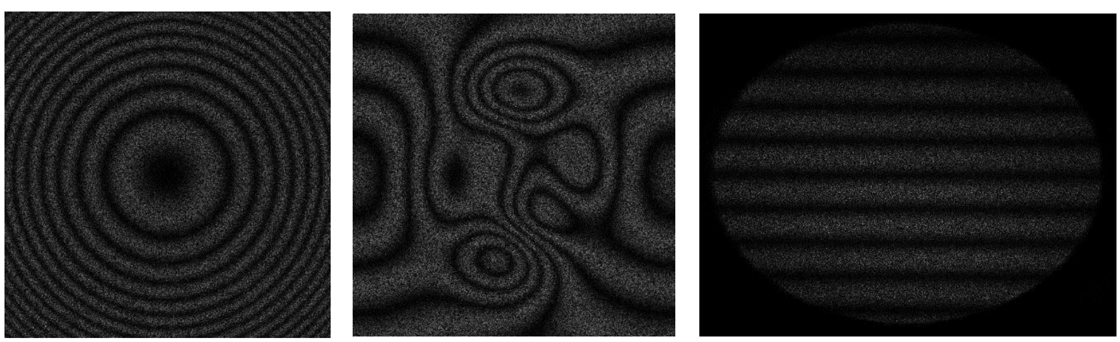

(a) (b) (c)

Fig 3. (a) and (b) Simulated speckle noise corrupted fringe patterns and (c) experimentally recorded fringe pattern in an ESPI setup corresponding to the in-plane displacement of an aluminium plate.

Table 1. Fringe denoising performance metrics: image fidelity and speckle index

	IF/SI			
	PDE	**WFF**	**DR**	**Proposed**
Fig 3 (a)	0.3572/**0.1013**	0.3710/0.1318	0.3674/0.1204	**0.9242**/0.3446
Fig 3 (b)	0.3993/0.0877	0.4032/0.1175	0.3803/**0.0637**	**0.9788**/0.2388

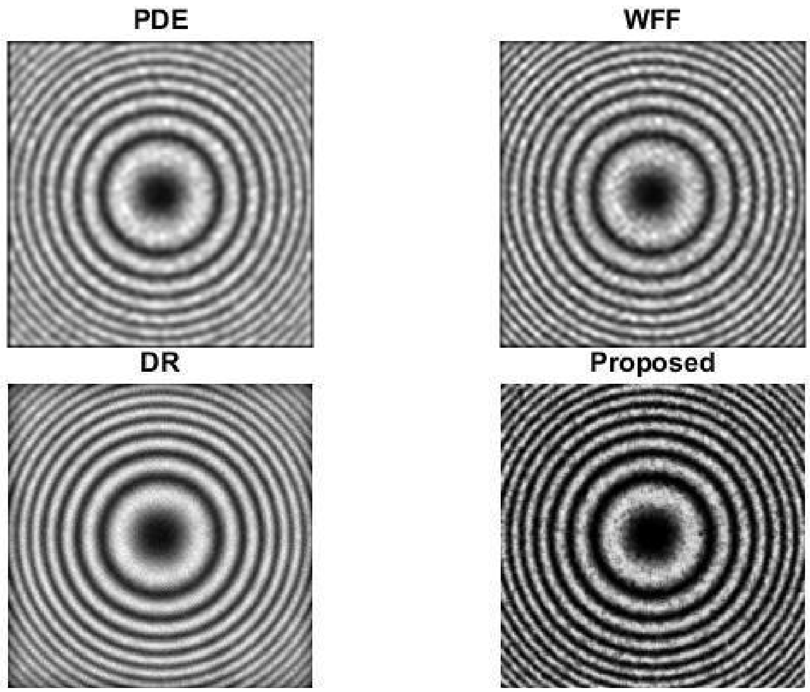

Fig 4. Denoising results obtained using PDE, WFF, DR, and the proposed technique for the fringe pattern example given in Fig 3 (a).

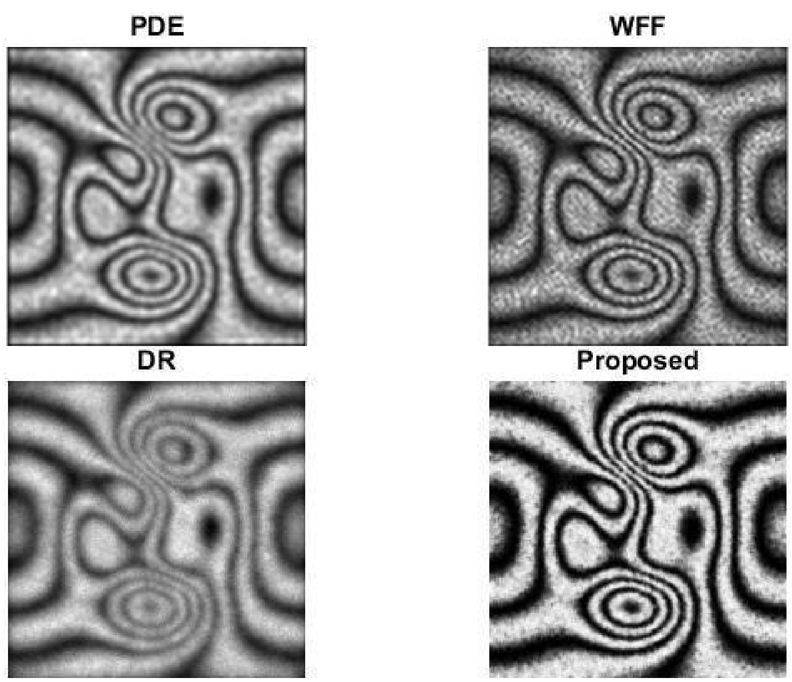

Fig 5. Denoising results obtained using PDE, WFF, DR, and the proposed technique for the fringe pattern example given in Fig 3 (b).

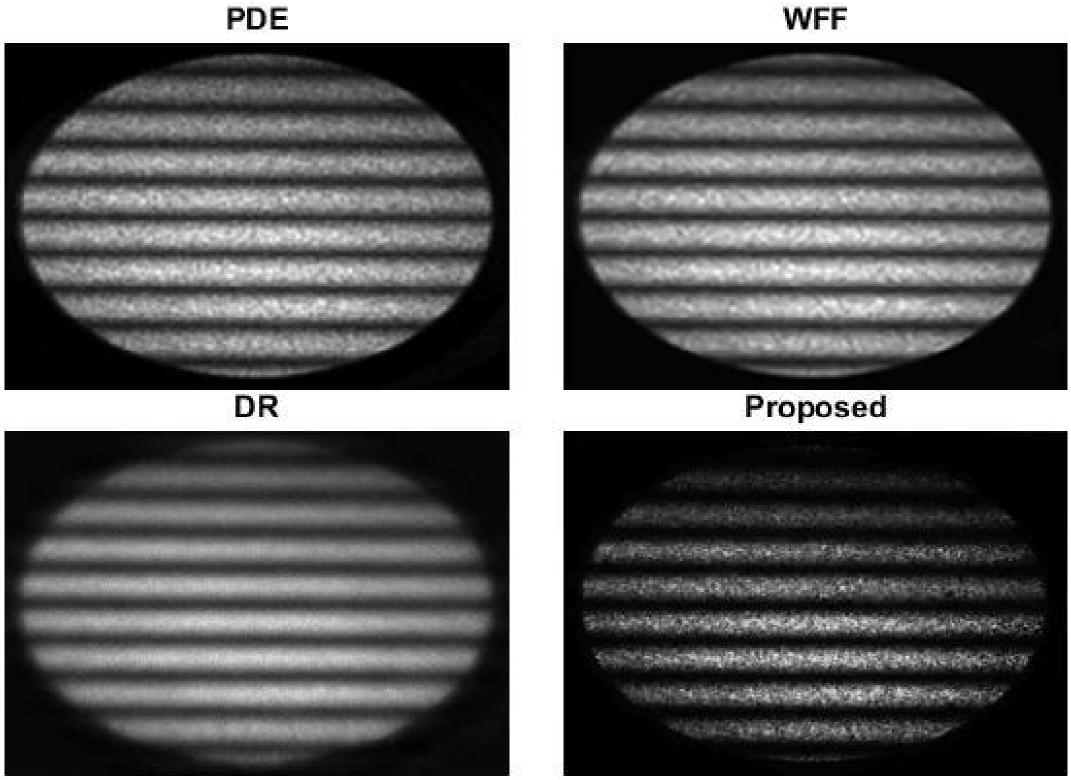

Fig 6. Denoising results obtained using PDE, WFF, DR, and the proposed technique for the fringe pattern shown in Fig 3 (c).

Experimental validation of the proposed algorithm is performed using the fringe pattern recorded in an ESPI setup corresponding to the in-plane displacement of an aluminium plate shown in Fig 3 (c). It can be deduced from the result given in Fig 6 that the proposed algorithm is capable of providing satisfactory performance in the fringe denoising.

4 Conclusion

An appropriately trained CNN architecture is found to provide acceptable fringe denoising performance even with a simple model architecture. Since the proposed fringe denoising algorithm does not consider any assumption on the fringe frequencies, it can prove to be a powerful candidate for fringe denoising in the practical applications. It can be expected that further increase in the model complexity may improve the denoising performance especially in the context of local fringe smoothing.

References

1. Rastogi P (ed), Digital Speckle Pattern Interferometry and Related Techniques, (Wiley N Y), 2001.
2. Kulkarni R, Rastogi P, Single and Multicomponent Digital Optical Signal Analysis, (IOP Publishing), 2017.
3. Servin M J, Quiroga A J, Padilla M, Fringe Pattern Analysis for Optical Metrology: Theory, Algorithms, and Applications, (Wiley-VCH), 2014.
4. Yu Q, Sun X, Liu X, Spin filtering with curve windows for interferometric fringe patterns, *Proc SPIE*, 4537(2002)358-361.
5. Yu Q, Sun X, Liu X, Removing speckle noise from speckle fringe patterns by spin filtering with curved surface windows, *Proc SPIE*, 4664(2002)73-79.

6. Cheng L, Tang C, Yan S, Chen X, Wang L,Wang B,New fourth order partial differential equations for filtering in electronic speckle pattern interferometry fringes, *Opt Commun*, 284(2011)5549-5555.
7. Mi Q-h, Yan S, Tang C, Numerous possible oriented partial differential equations and investigation of their performance for optical interferometry fringes denoising, *Appl Opt*, 52(2013)8439-8450.
8. Xu W, Tang C, Gu F, Cheng J, Combination of oriented partial differential equation and shearlet transform for denoising in electronic speckle pattern interferometry fringe patterns, *Appl Opt*, 56(2017)2843-2850.
9. Kerr D, Mendoza-Santoyo F, Tyrer J R, Manipulation of the Fourier components of speckle fringe patterns as part of an interferometric analysis process, *J Mod Opt*, 36(1989)195-203.
10. Federico A, Kaufmann G H, Comparative study of wavelet thresholding methods for denoising electronic speckle pattern interferometry fringes, *Opt Eng*, 40(2001)2598-2604.
11. Mirza S, Kumar R, Shakher C, Study of various pre-processing schemes and wavelet filters for speckle noise reduction in digital speckle pattern interferometric fringes, *Opt Eng*, 44(2005)1-6.
12. Tounsi Y, Ghlaifan A, Kumar M, Mendoza-Santoyo F, Matoba O, Nassim A, Fringe pattern analysis in wavelet domain. in, Holographic Materials and Applications, (ed) Kumar M, Chapt 8, (Intech Open, Rijeka), 2019.
13. Kemao Q, Windowed Fourier transform for fringe pattern analysis, *Appl Opt*, 43(2004)2695-2702.
14. Vargas J, Sorzano C O S, Quiroga J A, Estrada J C, Carazo J M, Fringe pattern denoising by image dimensionality reduction, *Opt Lasers Eng*, 51(2013)921-928.
15. Maciej W, Krzysztof P, Denoising and extracting background from fringe patterns using midpoint-based bidimensional empirical mode decomposition, *Appl Opt*, 53(2014)B215-B222.
16. Tounsi Y, Kumar M, Nassim A, Mendoza-Santoyo F, Speckle noise reduction in digital speckle pattern interferometric fringes by nonlocal means and its related adaptive kernel-based methods, *Appl Opt*, 57(2018)7681-7690.
17. Tang C, Wang L, Yan H, Li C, Comparison on performance of some representative and recent filtering methods in electronic speckle pattern interferometry, *Opt Lasers Eng*, 50(2012)1036-1051.
18. Kulkarni R, Rastogi P, Fringe denoising algorithms: A review, *Opt Lasers Eng*, (2020)106190; doi.org/10.1016/j.optlaseng.2020.106190.
19. Cai Y, Liang J, Yu X, A novel automated approach for noise detection in interference fringes pattern images using feature learning, *Proc SPIE*, 10835(2018); doi.org/10.1117/12.2505200
20. Chen M, Tang C, Xu M, Lei Z, A clustering framework based on FCM and texture features for denoising ESPI fringe patterns with variable density, *Opt Lasers Eng*, 119(2019)77-86.
21. Hao F, Tang C, Xu M, Lei Z, Batch denoising of ESPI fringe patterns based on convolutional neural network, *Appl Opt*, 58(2019)3338-3346.
22. Yan K, Yu Y, Huang C, Sui L, Qian K, Anand A, Fringe pattern denoising based on deep learning, *Opt Commun*, 437(2019)148-152.
23. Feng S, Chen Q, Gu G , Tao T, Zhang L, Hu Y, Yin W, Zuo C, Fringe pattern analysis using deep learning, Advanced Photonics, 1(2019)025001; doi.org/10.1117/1.AP.1.2.025001.

[*Received*: 02.08.2020; *accepted*: 24.08.2020]